GLIA

WILEY

RESEARCH ARTICLE

Microglial angiotensin type 2 receptors mediate sex-specific expression of inflammatory cytokines independently of circulating estrogen

Pablo Garrido-Gil[1,2] | Maria A. Pedrosa[1,2] | Maria Garcia-Garrote[1,2] |
Ana Pequeño-Valtierra[3] | Jorge Rodríguez-Castro[3] | Daniel García-Souto[3] |
Ana I. Rodríguez-Pérez[1,2] (iD) | Jose L. Labandeira-Garcia[1,2] (iD)

[1]Laboratory of Cellular and Molecular Neurobiology of Parkinson's disease, Research Center for Research in Molecular Medicine and Chronic Diseases (CIMUS), Department of Morphological Sciences, IDIS, University of Santiago de Compostela, Santiago de Compostela, Spain

[2]Networking Research Center on Neurodegenerative Diseases (CiberNed), Madrid, Spain

[3]Laboratory of Genomes and Disease, Center for Research in Molecular Medicine and Chronic Diseases (CIMUS), University of Santiago de Compostela, Santiago de Compostela, Spain

Correspondence
Jose L. Labandeira-Garcia and Ana I. Rodríguez-Pérez, Department of Morphological Sciences, CIMUS, University of Santiago de Compostela, 15782 Santiago de Compostela, Spain.
Email: joseluis.labandeira@usc.es and anai.rodriguez@usc.es

Abstract

There are sex differences in microglia, which can maintain sex-related gene expression and functional differences in the absence of circulating sex steroids. The angiotensin type 2 (AT2) receptors mediate anti-inflammatory actions in different tissues, including brain. In mice, we performed RT-PCR analysis of microglia isolated from adult brains and RNA scope in situ hybridization from males, females, ovariectomized females, orchiectomized males and brain masculinized females. We also compared wild type and AT2 knockout mice. The expression of AT2 receptors in microglial cells showed sex differences with much higher AT2 mRNA expression in females than in males, and this was not dependent on circulating gonadal hormones, as observed using ovariectomized females, brain masculinized females and orchiectomized males. These results suggest genomic reasons, possibly related to sex chromosome complement, for sex differences in AT2 expression in microglia, as the AT2 receptor gene is located in the X chromosome. Furthermore, sex differences in expression of AT2 receptors were associated to sex differences in microglial expression of key anti-inflammatory cytokines such as interleukin-10 and pro-inflammatory cytokines such as interleukin-1β and interleukin-6. In conclusion, sex differences in microglial AT2 receptor expression appear as a major factor contributing to sex differences in the neuroinflammatory responses beyond the effects of circulating steroids.

KEYWORDS
AT2 receptor, gender, gonadal hormones, interleukins, neuroinflammation, sex chromosome complement, sex dimorphism

---

Pablo Garrido-Gil and Maria A. Pedrosa contributed equally to experiments.

----

1 | INTRODUCTION

It is now known that sex modifies the outcome of many neurological diseases and particularly those related to neuroinflammation (Mazure & Swendsen, 2016; Villapol et al., 2017). Several studies have shown that microglial cells show sex differences, and this may play a major role in sex differences in disease outcome (Han et al., 2021; Kerr et al., 2019). Initially, sex differences were related to effects of circulating gonadal hormones, particularly on microglial inflammasome (Habib & Beyer, 2015). Microglial cells respond to in vitro treatments with gonadal steroids and changes in neuroinflammatory or neurodegenerative responses were observed after ovariectomies (Acosta-Martinez, 2020; Rodriguez-Perez et al., 2011, 2012; VanRyzin et al., 2019). However, a series of recent studies have revealed that other factors, more difficult to identify in classic in vitro studies, may also determine sex differences in microglia. Microglia can maintain sex-related gene expression and functional differences in the absence of circulating sex steroids (Bordt et al., 2020; Villa et al., 2018). It has been suggested that hormones may act during very early stages of brain development, leading to permanent sex-related changes in microglia (Hanamsagar et al., 2017; Villa et al., 2016). Recent studies also suggest the primary action of genes located in the sex chromosomes, so that hormones may be considered as the most important secondary factor downstream of primary effects of sex chromosomes (Arnold, 2020). Incomplete X chromosome inactivation may lead to double expression of some genes leading to sex differences in the related functions (Syrett & Anguera, 2019; Tukiainen et al., 2017), including inflammatory responses (Qi et al., 2021). Most of the escape genes lie in the Xq region, which is the older evolutionary region of the chromosome (Ross et al., 2005).

The angiotensin type 2 (AT2) receptors mediate anti-inflammatory actions in different tissues, including brain (Bhat et al., 2019; Fatima et al., 2021). In the brain, AT2 receptors have been observed in neurons and glial cells of rodents, monkeys and humans (Garrido-Gil et al., 2013, 2017), and promote neuroprotective and anti-inflammatory effects, inducing a shift from pro-inflammatory to anti-inflammatory microglial phenotypes (Jackson et al., 2020; Rodriguez-Perez et al., 2020). Interestingly, AT2 receptors were found overexpressed in several murine female tissues relative to males (Garrido-Gil et al., 2021; Okumura et al., 2005; Rodriguez-Perez et al., 2011), and the AT2 receptor gene is in the X chromosome, and particularly in the Xq23 region (de Gasparo et al., 2000). Therefore, both hormonal and sex chromosome complement effects may be responsible for primary sex differences in AT2 expression and differences in microglial responses.

In the present study, we isolated microglia from adult healthy mouse brains of males, females, ovariectomized (OVX) females, masculinized females and orchiectomized males, and from both wild type (WT) and AT2 knockout (KO) mice. In microglial cells from the different hormonal conditions, we studied the AT2 receptor expression and the expression of several interleukins (IL) that have previously been shown to be related with the AT2 receptor activity (IL-10, IL-6, and IL-1β). The *substantia nigra* has the highest levels of microglia in healthy mouse brains (Lawson et al., 1990), and was used to further confirm the presence of AT2 receptors in microglial cells using RNA scope in situ hybridization.

2 | METHODS

2.1 | Experimental design

Young adult (2–4-month-old) male and female wild-type (WT) and AT2 receptor knockout (AT2 KO; generous gift of Dr. Daniel Henrion) C57/BL6 mice were used. Animals were housed in conditions of constant room temperature (21–22°C) and a 12:12 h light–dark cycle and given free access to food and water. All experiments were carried out in accordance with the European Directive 2010/63/EU and the Spanish RD/53/2013 and were approved by the corresponding Ethics Committee at the University of Santiago de Compostela.

A first series of experiments were performed in WT mice. In a group of mice, adult microglial cells were isolated from brains of male ($n = 14$), female ($n = 14$) and ovariectomized (OVX)-female ($n = 14$) WT mice and were used to study the effect of sex and estrogen on the AT2 receptor and anti-inflammatory (IL-10) and pro-inflammatory (IL-1β, IL-6) cytokine mRNA expression. Two mouse brains were used to obtain one sample of microglial cells. A second group of male ($n = 8$) and female ($n = 8$) WT mice were quickly perfused with ice-cold saline and brains extracted and processed for microglial isolation, as controls to exclude any contamination by circulating blood cells. An additional group of male ($n = 10$) and female ($n = 10$) WT mice were included to observe the mRNA expression of AT2 receptors in microglial cells in brain tissue sections containing the *substantia nigra* by RNA scope in situ hybridization (both double in situ or immuno/in situ labeling).

In a second series of experiments, adult microglia were isolated from male AT2 KO mice ($n = 14$), female AT2 KO mice ($n = 14$) and ovariectomized female AT2 KO mice ($n = 14$) to evaluate the effect of AT2 receptor on sex- and estrogen-related differences in pro- and anti-inflammatory cytokine expression.

A third series of mice were used to observe the response of above mentioned IL to a pro-inflammatory stimulus in the presence and absence of AT2 receptors: WT female mice ($n = 4$) and AT2 KO female mice ($n = 4$) were treated with LPS or vehicle ($n = 4$) and sacrificed 24 h later for microglia extraction.

In additional series of mice, other possible mechanisms involved in sex differences observed in microglial AT2 receptor expression were investigated. First, male mice were bilaterally orchiectomized ($n = 6$) to analyze possible effects of male gonadal hormones. Second, female pups ($n = 11$) were subjected to brain masculinization using subcutaneous injections of estradiol benzoate. Finally, microglial cells isolated from wild type females ($n = 3$) and males ($n = 3$) were used to study the possibility of observing sex differences in the methylation status in the promoter of the AT2 gene (*Agtr2*).

2.2 | Estrogen depletion by ovariectomy and ELISA analysis

Female mice were bilaterally ovariectomized through a dorsal incision as previously described (Garrido-Gil et al., 2021). The anesthetized animal was placed in the prone position with the tail facing the

surgeon and the dorsal surgical area was shaved and cleaned with povidone iodine. A skin incision was made at the level of the midline between the caudal edge of the rib cage and the base of the tail. Then, an incision (bilateral to the spinal column) was made in the muscle wall. The ovaries were then located and removed outside. A sterile silk ligation was placed around the ovary, and it was removed. Finally, the muscle wall was closed with stitches, and the skin with staples. The animals were injected with atipamezole to promote their recovery, and with buprenorphine as an analgesic. Microglia was isolated 4 weeks after the operation.

17β-estradiol levels were quantified (pg/ml) in female (OVX, and non-OVX) and male mouse serum using a specific enzyme-linked immunosorbent assay (ab108667) from Abcam, following the manufacturer's instructions. Briefly, 17β-estradiol was added to standard, controls, and samples in the respective 96-well microtiter plates supplied by manufacturer and incubated for 2 h at 37°C. When incubation was completed, the wells were washed, and TMB substrate solution was added and incubated at room temperature in the dark. After that, stop solution was added and the absorbance of the samples was read at 450 nm in an Infinite M200 multiwell plate reader (TECAN).

2.3 | Brain masculinization, male orchiectomy, and LPS treatment

Brain masculinization was carried out by subcutaneous injections of 5 mg of 17β-estradiol benzoate (E8515, Sigma) dissolved in 50 ml of sterile sunflower oil. Male and female pups ($n = 11$) were injected at days P2, P5, and P8 (Villa et al., 2018). The effectiveness of the intervention was tested by microscopic evaluation of the types of cells present in vaginal smears, a common procedure used to document the stages of the estrous cycle (Cora et al., 2015). The masculinized females were unable to cycle at 8 weeks of age.

Male mice were bilaterally orchiectomized ($n = 6$) through a small incision at the tip of the scrotum. Anesthetized animals were immobilized, shaved, and disinfected. The tunic was opened, and the testis and epididymis were exteriorized. After placing a sterile silk ligation around the caudal zone of the spermatic cord, the testis and epididymis were removed, and the remaining tissue returned into the sac. The procedure was repeated with the other testis. Finally, the muscle wall was closed with stitches, and the skin with staples. In sham orchiectomized animals ($n = 6$) scrotal sac was opened without removing the testis. Finally, the incision was closed, and sutured. Animals were allowed to recover for 2 weeks before study. Testosterone levels were quantified in sham (i.e., controls, $n = 6$) and in orchiectomized mice ($n = 6$) serum using a specific competitive enzyme-linked immunosorbent assay (ADI-900-065 from Enzo), following strictly the manufacturer's instructions. Optical density was measured at 405 nm (with correction at 570 nm) using an Infinite M200 multiwell plate reader (TECAN; 2.0 software) and testosterone concentrations were quantified using a specific standard curve (4PL curve fit). Testosterone levels were 4.393 ng/ml ± 0.404 (SEM) in sham-operated mice and 0.513 ng/ml ± 0.0289 (SEM) in orchiectomized mice.

To observe the response to the LPS pro-inflammatory stimulus in the presence and absence of AT2 receptors, WT female mice ($n = 4$) and AT2 KO female mice ($n = 4$) were treated with LPS (lipopolysaccharide; 5 mg/kg i.p.; Sigma) and sacrificed 24 h later, as previously described (Rodriguez-Perez et al., 2020). The control group were WT female mice treated with sterile saline solution ($n = 4$).

Finally, microglial cells isolated from a group of male ($n = 3$) and female ($n = 3$) mice were used to study possible sex differences in the methylation status in the promoter of the AT2 gene (*Agtr2*).

2.4 | Adult microglia isolation

Isolation of adult microglia from mouse brains was performed as previously described (Rodriguez-Perez et al., 2020) with slight modifications. Two mouse brains were used to obtain one sample of microglial cells. Brains from perfused (ice-cold saline; 0.9% in DEPC water) or non-perfused mice were removed and washed in free-serum DMEM/F12 with penicillin/streptomycin and glucose. Then, each brain hemisphere was fully minced with a scalpel into small pieces (approximate 1 mm^2), repeatedly washed to remove blood cells from vessels, transferred to a Dounce homogenizer containing 5 ml of the enzymatic mix (1 mg/ml papain, 6 U/ml dispase and 20 U/ml DNase in a DMEM/F12 solution with 12.5 mM HEPES and 37.5 mM NaCl) and dissociated on ice with 10–12 passes using the loose-fitting pestle. Dissociated tissue was transferred to a 50 ml conical tube and the enzymatic digestion was performed at 37°C for 30 min. Then, cell suspension was washed with 10 ml of ice-cold Hanks' balanced salt solution (HBSS), filtered (100 μm cell strainer) and centrifuged (300 g at 4°C for 5 min). The pellet was resuspended in 8 ml of 35% Percoll at RT and transferred to a clean conical tube. After overlaying with 5 ml of HBSS, each sample was incubated for 5 min on ice, and centrifuged (800 g at 4°C for 20 min) without braking. Then, the cellular pellet was washed with HBSS, filter (30 μm), centrifuged (400 g at 4°C for 5 min), and subsequently, resuspended in 90 μl of separation buffer (PBS with 0.5% bovine serum albumin and 2 mM EDTA), and was transferred to a 15 ml conical tube. For microglia isolation, 10 μl of CD11b (Microglia) MicroBeads (130-093-634, MACS Miltenyi Biotec) were added, and then, the cell-bead suspension was incubated (15 min at 4°C) under agitation, washed, resuspended in 500 μl of separation buffer and applied onto MS columns (130-042-210, MACS Miltenyi Biotec) according to manufacturer instructions.

2.5 | Flow cytometry analysis

Microglial cells isolated by magnetic sorting were incubated (15 min at 4°C) under agitation with monoclonal antibodies against CD11b (PE-conjugated: eBioscience 12-0112, 1:170), CD45 (FITC-conjugated: eBioscience 11-0451, 1:200) or isotype controls (eBioscience 12-4331, 1:50, and 11-4331, 1:100). Then, cells were rinsed in 2 ml ice-cold PBS, pelleted at 300 g for 10 min at 4°C and resuspended in 300 μl of separation buffer. To discriminate between living and dead

cells, cells were incubated with DAPI 10 min before flow cytometry. Cells were analyzed on an Accuri C6 flow cytometer (BD Biosciences). For each staining condition (cells only, isotype control, and antibody of interest), at least 1×10^4 events were collected and then analyzed using a FlowJo v10 software (BD Biosciences). Microglia purity was defined as the percentage of all living CD11b+ cells that showed CD45 low expression. Positive labeled cells were determined by setting threshold on background staining of isotype control.

2.6 | Real time quantitative PCR

Firstly, total RNA extraction was performed with the RNeasy minikit (Qiagen) protocol and then, the RNA was reverse transcribed to complementary DNA using the high-capacity RNA-to-cDNA kit (4387406, Applied Biosystems). Subsequently, the real time qPCR analysis was performed with a QuantStudio3 platform (Applied Biosystems) and the EvaGreen qPCR MasterMix (Applied Biological Materials Inc.). β-actin was used as housekeeping gene and was amplified in parallel with the genes of interest. The relative levels of mRNA were evaluated by the delta Ct method ($2^{-\Delta\Delta Ct}$), where Ct is the cycle threshold. Expression of each gene was obtained as relative to that of the housekeeping transcripts. Forward (F) and reverse (R) primers sequences, designed using Beacon Designer software (Premier Biosoft), were as follows: for β-actin, F 5′-TCGTGCGTGACATTAAAGAG-3′, R 5′-TGC CACAGGATTCCATACC-3′; for AT2, F 5′-TGTGGTCTCACTGTTTT GTTGTCA-3′, R 5′-TTGCCCAGAGAGGGAGGGTA-3′; for IL-1β, F 5′- CCGTGTCTTCCTAAAGTATGG-3′, R 5′-GTTTCTTGTGACCCTG AGC-3′; for IL-6, F 5′-GACTGATGCTGGTGACAAC-3′, R 5′-GAGT GGTATCCTCTGTGAAGT-3′; and for IL-10, F 5′-CATACTGCTAACCG ACTC-3′, R 5′-AATGCTCCTTGATTTCTGG-3′.

2.7 | RNA scope in situ hybridization

Brains from adult mice were rapidly removed, embedded in OCT, frozen with liquid nitrogen cooled-isopentane, and stored at −80°C. Then, coronal sections (15 μm thick) containing the *substantia nigra* were cut at −20°C with a cryostat (Thermo Scientific), mounted on glass slides (Superfrost Plus, Thermo Fisher Scientific), and stored at −80°C until use. Tissue collection and sectioning were performed in RNase free conditions.

For in situ hybridization, slides containing nigral tissue sections were processed with the RNAscope Fluorescent Multiplex Assay using the RNAscope® Fluorescent Multiplex Reagent Kit (320293-USM; Advanced Cell Diagnostics, ACD, Newark, CA), according to the manufacturer's instructions. Tissue sections were fixed with 4% paraformaldehyde for 30 min at 4°C, dehydrated in graded ethanol (50%, 70%, and 100% for 5 min each step) and incubated with Protease IV (322340, ACD) for 30 min at RT. Then, hybridization was performed into the ACD HybEZ™ II oven (321720, AC) at 40°C for 2 h using the following target probes: *Mus musculus* angiotensin II receptor type 2 mRNA (*Agtr2* probe; accession number NM_007429.5, target region

397-1697; 406471-C2, ACD) and *Mus musculus* integrin alpha M (*Itgam*), transcript variant 1, mRNA (accession number NM_001082960.1, target region 538-1528; 311491 -C3, ACD), as a microglial marker. In addition, RNAscope 3-plex Negative Control Probe_Mm (320871, ACD) and RNAscope 3plex Positive Control Probe_Mm (320881, ACD) were used as control probes. After probes hybridization, the tissue sections were sequentially incubated into the ACD HybEZ™ II oven at 40°C with amplification reagents (Detection Reagents kit, 320851, ACD): AMP-1 for 30 min, AMP-2 for 15 min, AMP-3 for 30 min and AMP-4 C for 15 min, which assigned the different fluorophores to each channel: *Agtr2* probe (channel 2; fluorophore: Atto 647), *Itgam* (channel 3; Alexa 488). Then, tissue sections were incubated with DAPI (320858, ACD) for 30 s at RT and immediately cover slipped with Fluoromount-G™ Mounting Medium (00-4958-02, Invitrogen).

2.8 | RNA scope in situ hybridization combined with immunohistochemistry

The combination of the RNA scope in situ hybridization technique and the immunofluorescence technique was performed as previously described (Lanfranco et al., 2017; Villapol et al., 2017), with slight modifications. For tissue preparation, mice were first transcardially perfused with 0.9% saline and then with cold 4% paraformaldehyde in 0.1 M PBS (pH 7.4). The brains were removed, washed and cryoprotected in PBS containing 20% sucrose (24 h at 4°C). Brains were embedded in OCT and frozen with liquid nitrogen cooled-isopentane. Then, coronal tissue sections (15 μm thick) were cut with a cryostat (Thermo Scientific), mounted on glass slides (Epredia™ Polysine Adhesion Slides, Thermo Fisher Scientific), and stored at −80°C until use.

Fluorescent in situ hybridization was performed using RNA scope® Technology 2.5 Red fluorescent kit for fixed tissue (Advanced Cell Diagnostics, ACD; Hayward, CA), according to the manufacturer's instructions. Briefly, tissue sections were incubated (30 min at 60°C) in a HybEZTM II oven (321720, AC), pretreated (10 min at RT) with a H_2O_2 solution (322335, ACD) and boiled (5 min) with RNA scope Target Retrieval (322001, ACD). Then tissue sections were washed in 100% ethanol and incubated with Protease Plus (322331, ACD) for 30 min at 40°C. In situ hybridization was performed using a Mus musculus angiotensin II receptor type 2 mRNA probe (Agtr2; accession number NM_007429.5, target region 397-1697; 403991-C1, ACD) for 2 h at 40°C. Then, sequential amplification steps were performed at 40°C (Detection Reagent-RED kit, 322360, ACD). Finally, tissue sections were incubated with a detection solution containing a mixture ratio of Red-A to Red-B of 1:60. Positive hybridization consisted of a punctate signal in the far-red spectrum (Excitation: 647 nm; Emission: 657–727 nm) representing a single mRNA target molecule.

Following in situ hybridization, tissue sections were processed for immunofluorescence for the microglial marker Iba1. In short, post-hybridized sections were first blocked with 5% normal donkey serum (Sigma) in PBS-tween for 1 h at RT and then incubated overnight at 4°C with a rabbit polyclonal antibody against Iba-1 (1:100; 019-19741, Wako). The immunoreaction was visualized with an Alexa

fluor 488-conjugated donkey anti-rabbit IgG (1:200, 2 h at RT; Molecular Probes, Eugene, OR). Finally, tissue sections were incubated with DAPI (320858, ACD) for 30 s at RT and immediately cover slipped with Fluoromount-G™ Mounting Medium (00-4958-02, Invitrogen).

2.9 | Images acquisition and quantitative analysis

Tissue sections processed for RNA scope in situ hybridization alone or in combination with immunofluorescence technique were visualized using a confocal laser scanning microscope (AOBS-SP5X; Leica Microsystems Heidelberg GmbH, Mannheim, Germany). Fluorescent signals of AT2 mRNA and CD11b mRNA hybridization and immunofluorescence for Iba1 were imaged with a 40× and 63× objective lens.

For quantitative analysis, three _substantia nigra_ sections from each animal ($n = 5$ per group), selected throughout its anteroposterior axis (anterior, central, and posterior levels) were analyzed by investigators blinded to experimental conditions. Images from six microscopic fields (40× 0.15 mm^2 by field) per each tissue section were obtained within the _substantia nigra_ by laser scanning microscopy and using constant microscope parameters and similar laser intensity. The total number of microglial cells and the total number of microglial cells that express AT2 mRNAs were quantified using the ImageJ64 software (National Institute of Health. Bethesda, MD, USA). Only cell profiles showing a labeled nucleus and microglial morphology were included. The negative probe used as a control did not contain any

stained cells. Data were presented as the mean number of cells per mm^2. The percentage of microglial cells expressing AT2 mRNA was calculated from the corresponding absolute values. In addition, the number of AT2 mRNA positive dots per each cell was quantified in these microscopic fields to assess the intracellular mRNA levels of AT2. A total of 60 microglial cells per animal were analyzed using the ImageJ64 software.

2.10 | Methylation status on the _Agtr2_ gene promotor

DNA was isolated from microglia from brains of male ($n = 3$) and female ($n = 3$) wild type mice and converted with sodium bisulfite using the EZ DNA Methylation-Gold Kit (Zymo Research; D5005) following the manufacturer recommendations. A set of PCR primers (MMU_AGTR2_met1L: 5′-TTAGAATTTTGTAGGTTGAAGGTTT-3′; MMU_AGTR2_met1R: 5′-CAAAATACAATTAAAATACAAAAAAAA-3′) was designed with Methprimer (Li & Dahiya, 2002) to amplify a 250 bp fragment encompassing the entire promoter of the AT2 receptor gene (_Agtr2_), as recovered from the Mus musculus reference genome (NC_000086.8). Next, we carried out PCR followed by Sanger and single-molecule sequencing of the resulting amplicons using a Seqstudio (Applied Biosystems) and a MinION (Oxford Nanopore Technologies Ltd, ONT), respectively. PCR conditions included 35 cycles of 95°C for 20 s, 50°C for 20 s and 72°C for 20 s, in a mix including 40 ng transformed DNA and 1× DreamTaq Hot Start Green
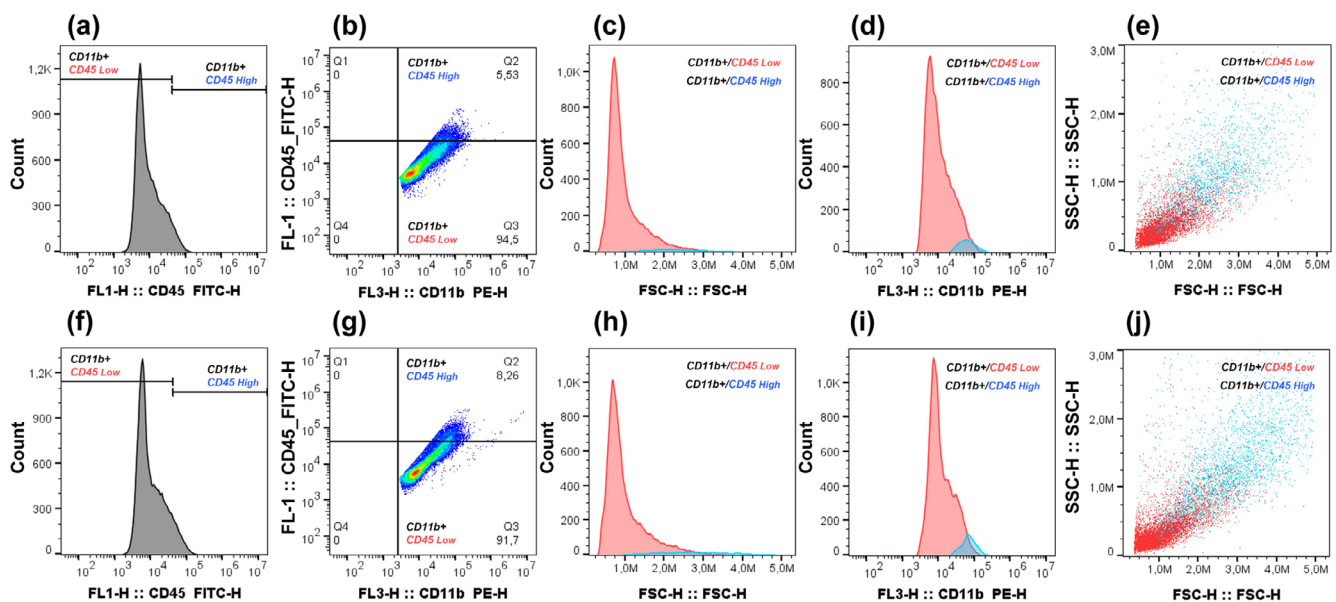

FIGURE 1 Flow cytometry analysis of the CD11b+ cells. Cells isolated from non-perfused [(a)–(e)] and perfused [(f)–(j)] brains did not show significant differences. [(a), (f)] Histograms showing two CD45-expressing cell populations: CD45 low (microglia) and CD 45 high (possible macrophages). [(b), (g)] Microglia, identified as CD11b+ and CD45 low (Q3), comprised the highest proportion of cells (91.7%–94.5%), whereas a low percentage of potential macrophages (CD11b+/CD45 high, Q2) were observed. [(c), (h)] Forward scatter (FSC) analysis showing a slight smaller size of the CD45 low cells (red) respect to CD45 high (blue) cells. [(d), (i)] CD11b analysis showed a slight lower expression within CD45 low cells (red) respect to CD45 high (blue) cells. [(e), (j)] Forward scatter (FSC) and side scatter (SSC) characteristics of CD11b+/CD45 low (red) and CD11b+/CD45 high (blue) are shown

PCR Master Mix (Thermo Scientific; MAN0015977). PCR amplicons were purified with ExoSAP-IT Express (Applied Biosystems; 75001.1. ML), amplified using the BigDye Terminator v3.1 kit (ThermoFisher; 4337455) and cleaned with BigDye XTerminator kit (ThermoFisher; 4376486) prior to Sanger sequencing in a SeqStudio genetic analyzer controlled by the Sequencing Analysis Software v6.0 (Applied Biosystems; 4474950). Electropherograms were trimmed, visualized and mapped to the reference sequence with Geneious. ONT libraries were constructed with the Sequencing 1D ligation kit (Oxford Nanopore Technologies Ltd; SQK-LSK109), including DNA repair with NEBNext FFPE DNA Repair Mix (New England BioLabs) and NEBNext Ultra II Ligation Module (New England BioLabs) and loaded onto MinION R9.4 flowcells (Oxford Nanopore Technologies Ltd; FLO-MIN106 rev-D), controlled by MinKNOW v19.12.5 and sequenced to $1000\times$ coverage. High accuracy base-calling was performed with Guppy v2.3.1 to generate fastq files and these were further mapped to the Mus musculus reference genome (NC_000086.8) with minimap2 v2.14-r88344. The resulting SAM files were processed with Samtools v1.744 and visualized with the Integrative Genome Viewer (IGV) to assess cytosine methylation status in the promotor and adjacent regions.

2.11 | Statistical analysis

All data were obtained from at least three independent experiments and were expressed as means ± SEM. Two group comparisons were performed with Student's t-test. Multiple comparisons were analyzed by one-way ANOVA (when one factor was studied) or two-way ANOVA (when two factors were studied), followed by Student–Newman–Keuls post-hoc test or the corresponding nonparametric test. The normality of populations and homogeneity of variances were tested before each ANOVA. Differences were considered statistically significant at $p \leq .05$. Statistical analyses were carried out with SigmaPlot 11.0 (Systat Software, Inc., San José, CA/USA). Statistics are detailed in Supplemental file 2: Table S1.

3 | RESULTS

3.1 | Characterization of models

First, we characterized our model of microglial isolation to confirm that the isolated CD11b+ cells were microglial cells and that the analyzed population was not constituted by other types of brain cells or blood cells. The efficacy of microglial isolation, confirmed by flow cytometry analysis of these CD11b+ cells, showed similar results when perfused (Figure 1a–e) or non-perfused (Figure 1f–j) brains were used for isolation.

Flow cytometry analysis showed two CD45-expressing cell subpopulations: CD45 low (microglia) and CD 45 high (possible macrophages) (Figure 1a,f). Microglia, identified as CD11b+ and CD45 low,

comprised the highest proportion of cells (91.7%–94.5%), whereas a low percentage of potential macrophages (CD11b+/CD45 high) were observed (Figure 1b,g). However, brain-resident microglia can upregulate CD45 expression in response to insults (Sedgwick et al., 1991), indicating difficulty to stablish that high CD45 are not microglia. The presence of these two cell populations was also confirmed by analysis of size (Figure 1c,h), CD11b expression levels (Figure 1d,i) and internal complexity (i.e., granularity) (Figure 1e,j). Thus, the microglia (CD11b+/CD45 low) showed a smaller size, a lower expression of CD11b and a lower internal complexity than CD11b+/CD45 high cells.
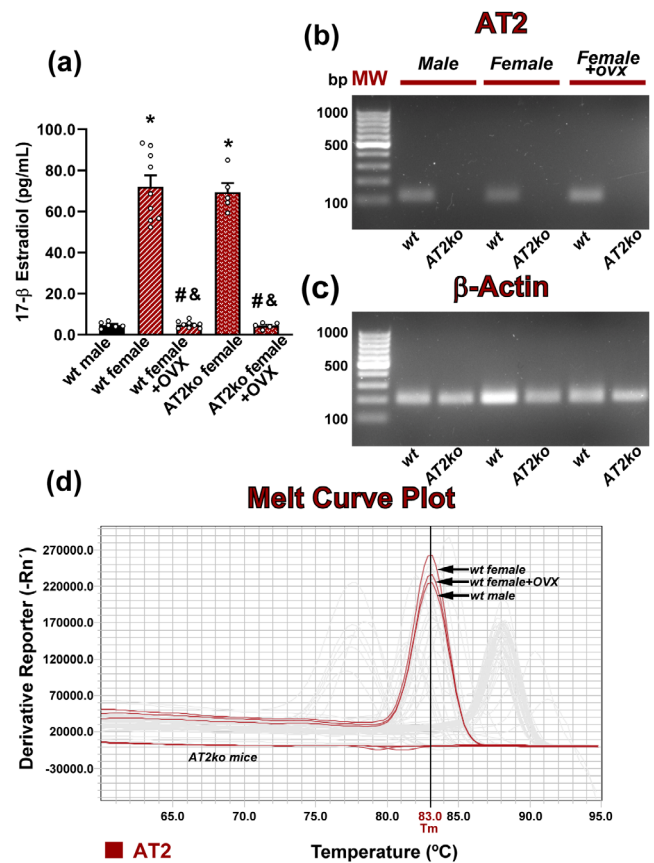

FIGURE 2 Estradiol concentrations (pg/ml) in different mouse groups and absence of AT2 mRNA in AT2 KO microglia. Estradiol (E2) serum concentrations in wild type (wt) males, wt females, ovariectomized (OVX) wt females, AT2 KO females and OVX AT2 KO females are shown in (a). The lack of expression of AT2 mRNA in adult microglia isolated AT2 KO mice and the presence in WT mice was demonstrated by RT-PCR [(b)–(d)]. Specific AT2 amplification by RT-PCR in adult microglia of WT mice was demonstrated by the presence of a unique peak at the corresponding melting temperature (T_m) in the melt curves, and no peak was observed in the melt curve plot of AT2 KO mice (d). Representative bands of AT2 expression by RT-PCR in isolated mouse WT and AT2 KO adult microglia [(b), (c)]. Data are mean ± SEMs. *$p < .05$ compared to male group, #$p < .05$ compared to wt female group, &$p < .05$ compared to AT2 KO females. Multiple comparisons were analyzed by Kruskal-Wallis one way analysis of variance on ranks followed by Dunn's method post-hoc test. KO, knockout; OVX, ovariectomized; wt, wild type

The levels of circulating estrogens in the different mouse models used in this study and efficacy of ovariectomies were estimated by determination of levels of Estradiol (E2) concentrations in wt males (4.658 ± 0.579 pg/ml), wt females (72.123 ± 5.526 pg/ml), ovariectomized (OVX) wt females (4.869 ± 0.551 pg/ml), AT2 KO females (72.702 ± 4.866 pg/ml) and OVX AT2 KO females (4.385 ± 0.645 pg/ml) (Figure 2a). These levels of E2 were similar to those obtained in our previous studies in mice (Garrido-Gil et al., 2021).

Then, we confirmed the specific AT2 amplification by RT-PCR in adult microglia. The specificity was demonstrated by the presence of a unique peak at the corresponding melting temperature (T_m) in the melt curves, while no peak was observed in the melt curve plot of the negative controls. The lack of AT2 receptors in the microglia isolated from AT2 KO mice was confirmed using primers designed against the mRNA region (second putative transmembrane domain) that is codified by the deleted sequence (exon 3) used for disrupting the *Agtr2* gene in these KO mice, which clearly showed that AT2 mRNA was expressed in microglia isolated from WT mice but was absent in microglia isolated from AT2 KO mice (Figure 2b–d).

3.2 | Levels of AT2 mRNA and inflammation-related cytokine expression in microglia from WT males and females

We analyzed the expression of AT2 mRNA and inflammation-related cytokines mRNA in microglial cells isolated from non-perfused (Figure 3a–d) and perfused (Figure 3e–h) brains of adult WT males, WT females and WT OVX females. AT2 mRNA expression was much higher in microglia from females and OVX females than in microglia from males (Figure 3a,e). There was a decrease in microglial AT2 expression in OVX females as compared with control females that was not statistically significant.

Microglia isolated from male brains showed lower levels of mRNA expression for the anti-inflammatory cytokine IL-10 than microglia from females and OVX females, and no significant difference was observed between females and OVX females (Figure 3b,f). However, mRNA expression for the pro-inflammatory cytokines IL-1β and IL-6 was significantly higher in microglia isolated from males than in microglia isolated from females or OVX females, and no significant differences in IL-1β and IL-6 expression were detected between females and OVX females (Figure 3c,d,g,h). These results were confirmed both
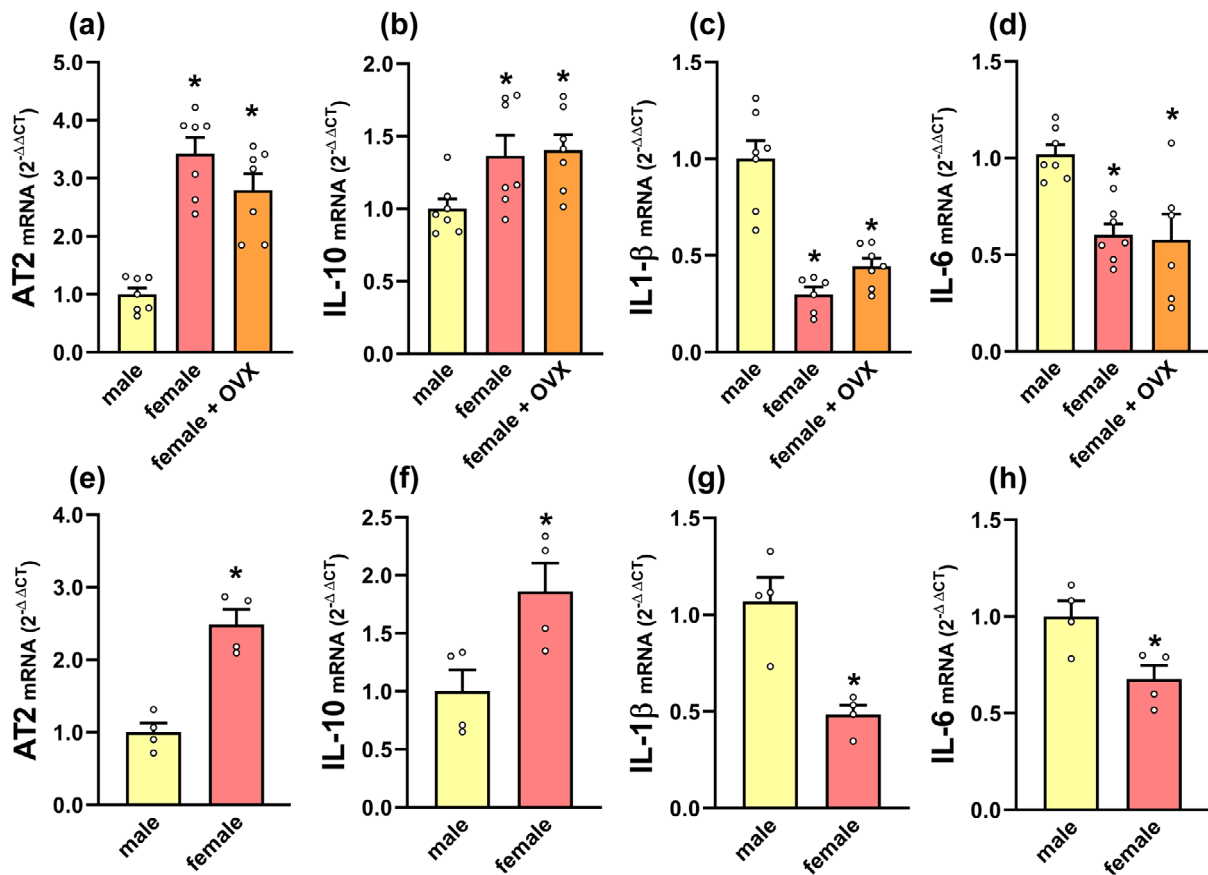

FIGURE 3 mRNA expression of AT2 [(a), (e)], IL-10 [(b), (f)], IL-1β [(c), (g)] and IL-6 [(d), (h)] in microglia. Microglia was isolated from perfused [(a)-(d)] and non-perfused [(e)–(h)] brains of wild type (WT) males, WT females and ovariectomized (OVX) WT females using RT-PCR. For mRNA the comparative cycle threshold values method ($2^{-\Delta\Delta Ct}$) was used. Data are mean ± SEMs. *$p < .05$ compared to wild type males. One-way ANOVA followed by Student's Newman–Keuls post-hoc test [(a)–(d)] and Student's *t* tests [(e)–(h)]

in perfused and non-perfused brains of WT mice indicating that these effects are not related to circulating macrophages. Altogether suggests that differences in expression of AT2 receptors, the anti-inflammatory cytokine IL-10 and the pro-inflammatory cytokines IL-1β and IL-6 in microglia of adult healthy WT mice are primary related to sex of mice.

Finally, we confirmed the expression of AT2 mRNA in microglia from healthy brains of WT male and female mice using in situ RNA scope in tissue sections from the nigral region, as well as in situ hybridization combined with immunohistochemistry (Figure 4). This again confirmed the presence of AT2 expression in cells labeled by microglial markers and showing clear microglial morphology (i.e., microglia) in control brains. As observed in isolated microglia, AT2 mRNA labeling was more marked in female than in male

microglia (Figure 4a–l). In situ procedures also showed that females had significantly higher number of AT2-labeled microglial cells, and significantly higher number of AT2 mRNA dots by cell than males (Figure 4m–p).

3.3 | Levels of inflammation-related cytokine expression in microglia from WT and AT2 KO males and females

In a second series of experiments, we used wild-type and AT2 KO males, females and OVX females to know whether differences in the microglial expression of IL-10, IL-1β and IL-6 between males and females (control or OVX females) and not dependent of circulating
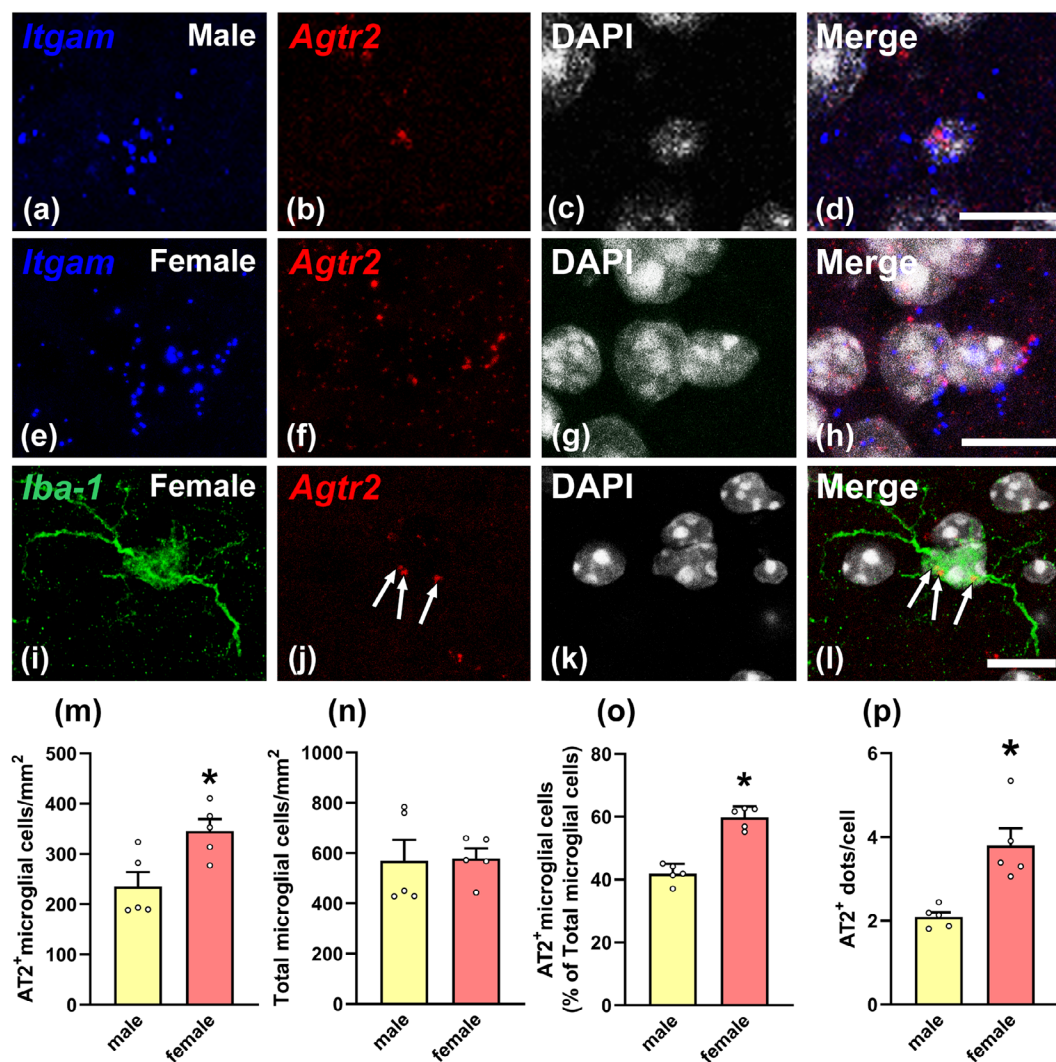

FIGURE 4 AT2 receptor mRNA expression using in situ RNA scope probes (Agtr2) and double immune/in situ RNA scope. Representative photomicrographs showing microglia from the nigral region in male [(a)–(d)] and female [(e)–(h)] wild-type (wt) mice using double in situ RNA scope (*Agtr2* in red and integrin alpha M, *Itgam* in blue), and counterstained with DAPI (white). [(i)–(l)] Double immuno/in situ showing Iba-1 (microglial marker; green) *and Agtr2* (red, arrows). [(m)–(p)] *Agtr2* was more abundant in microglia from females both in number (m), percentage (o) of labeled cells and dots by cell (p), without significant difference in the total number of microglial cells (n). Data are mean ± SEMs. *$p < .05$ compared to wt males. Student's *t* tests [(m)–(p)]. Scale bar 12.5 μm
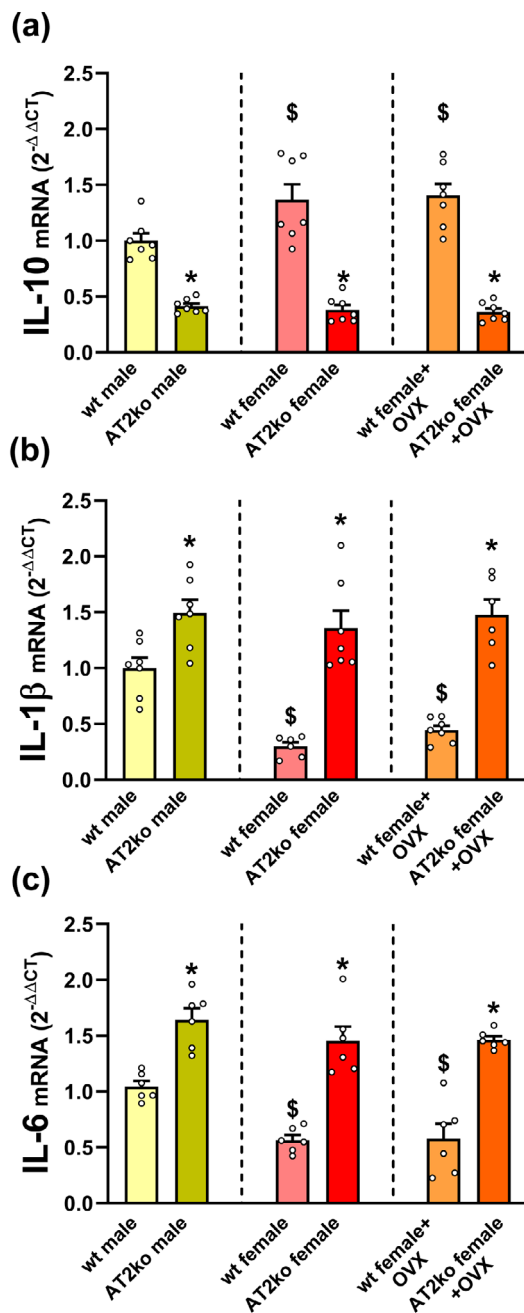
FIGURE 5 IL-10 (a), IL-1β (b), and IL-6 (c) mRNA in microglia isolated from different mouse groups. Wild-type (wt) or AT2 knockout (KO) male, female and ovariectomized (OVX) female brains were analyzed using RT-PCR. For mRNA, the comparative cycle threshold values method ($2^{-\Delta\Delta Ct}$) was used. Data are mean ± SEMs. *$p < .05$ compared to the corresponding wt control, $^{\$}p < .05$ compared to wt males. Multiple comparisons were analyzed by two-way ANOVA followed by Student–Newman–Keuls post-hoc test [(b), (c)] and two-way ANOVA on ranks Kruskal Wallis, (a)

gonadal steroids could be related to the observed differences in AT2 expression between males and females. Changes in IL-10, IL-1β, and IL-6 expression induced by AT2 deletion were more marked in females than in males, which is consistent with the higher levels of AT2 expression observed in females relative to males. Interestingly,
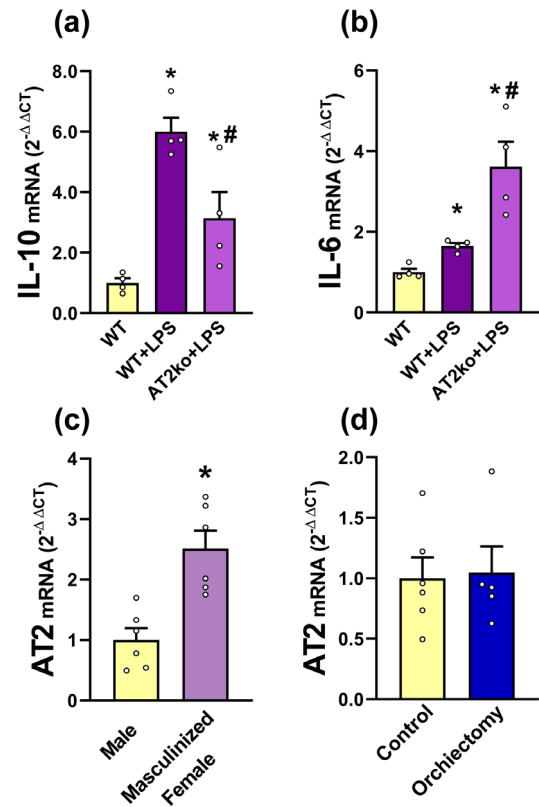

FIGURE 6 Effects of LPS injection on microglial interleukin mRNA expression in the presence or the absence of AT2 receptors (a, b), and effect of female brain masculinization (c) and male orchiectomy (d) on AT2 mRNA expression using RT-PCR. In vivo injection of LPS induced a marked increase in levels of IL-10 mRNA expression in microglia from WT mice that was much higher than in microglia from AT2 KO mice (a), while IL-6 mRNA expression was significantly higher in microglia from AT2 KO mice than in microglia from WT mice (b). Microglia from masculinized female brains showed higher AT2 mRNA expression than microglia from WT males (c). Microglia from orchiectomized WT males showed AT2 mRNA expression similar than microglia from control WT males (d). For mRNA, the comparative cycle threshold values method ($2^{-\Delta\Delta Ct}$) was used. Data are mean ± SEMs. *$p < .05$ compared to the corresponding WT control, $^{\#}p < .05$ compared to WT + LPS. One-way ANOVA followed by Student's Newman–Keuls post-hoc test (a); Kruskal-Wallis one way analysis of variance on ranks followed by Student's Newman–Keuls post-hoc test (b) and Student's t tests [(c), (d)]

no significant differences were observed in microglial expression of IL-10, IL-1β, and IL-6 between males, females and OVX females of AT2 KO mice, suggesting that differences in AT2 expression play a major role in sex differences in regulation of microglial IL-10, IL-1β, and IL-6 expression in the control brains (Figure 5a–c). Under intense pro-inflammatory stimulus with LPS, there was a marked increase in levels of mRNA expression for IL-10 in WT mice that was much higher than that observed in AT2 KO mice, while mRNA expression of the pro-inflammatory cytokine IL-6 was significantly higher in the AT2 KO mice relative to the WT mice (Figure 6a,b).

3.4 | Female brain masculinization or male orchiectomy do not change microgial AT2 mRNA expression. Methylation status in the promoter of the AT2 gene (*Agtr2*)

AT2 mRNA expression was significantly higher in microglia isolated from female masculinized brains relative to microglia from males, which does not support the possibility that the perinatal exposure to estrogens is responsible for the permanent increase in AT2 receptor expression in the microglia of females (Figure 6c).

AT2 mRNA expression was not significantly different in microglia isolated from brains of orchiectomized WT males relative to microglia from control WT males, which does not support the possibility that androgens are responsible for the sex differences by downregulating AT2 receptor expression in the microglia of males (Figure 6d).

Analysis of methylation status in the promoter of the AT2 gene (*Agtr2*) and adjacent regions did not show significant sex differences in CpG methylation. Details are shown in Supplemental file 1 (Figure S1). This suggests that mechanisms different to methylation may be responsible for sex differences in the regulation of the AT2 gene (see Discussion).

4 | DISCUSSION

In microglia isolated from healthy mouse brains, we confirmed the expression of AT2 receptors, although the expression is much lower in males than in females, and ovariectomy, orchiectomy or brain masculinization in females did not significantly affect this difference. In tissue sections, we also confirmed the presence of AT2 receptors in microglia of healthy brains using RNA scope in situ hybridization, which is consistent with our previous studies using immunohisto-chemistry (Garrido-Gil et al., 2013; Joglar et al., 2009). However, AT2 receptors were not found in microglia in other studies (de Kloet et al., 2016) or were suggested to be undetectable in vivo in healthy microglia and be upregulated in neuroinflammatory processes (Jackson et al., 2018). Specificity of commercial antibodies for AT2 has also been questioned by some studies (Hafko et al., 2013). These discrepancies are probably due to the use of modified animal models, male rodents and methods that differ in sensitivity for AT2 receptor.

AT2 receptors were shown to be protective in different tissues by antagonizing, via multiple signaling pathways, the pro-inflammatory effects induced by activation of the AT1 receptors (Bedecs et al., 1997; Bhat et al., 2019; Carey et al., 2000; Hakam & Hussain, 2006; Rodriguez-Perez et al., 2020). The anti-inflammatory role of AT2 receptor activation has been shown in a considerable number of studies in the brain and peripheral tissues (Bhat et al., 2019; Jackson et al., 2020; Matavelli et al., 2011; Rodriguez-Perez et al., 2020; Rompe et al., 2010), although the precise molecular mechanisms induced in different cell types remain to be totally clarified. The use of AT2 agonists (C21, CGP) and antagonists has shown that AT2 activation induces a decrease in NADPH-oxidase activity with the corresponding decrease in reactive oxygen species

(ROS) production, inhibition of nuclear factor kappa-light-chain-enhancer of activated B cells (NFκB) and extracellular signal-regulated protein kinases 1 and 2 (ERK1/2) phosphorylation, and that nitric oxide (NO) is a key second messenger for AT2 signaling (Bhat et al., 2019; Rodriguez-Perez et al., 2015; Wang et al., 2020; Zang et al., 2019).

We also analyzed the expression of several cytokines (IL-10, IL-6, IL-1β) that previous studies in different cells have shown to be closely related to the AT2 receptor activity. We observed that microglial expression of the anti-inflammatory cytokine IL-10 and pro-inflammatory cytokines IL-6 and IL-1β is different in microglia from control brains of males and females, which is not dependent on circulating gonadal hormones. However, these differences disappeared in AT2 KO mice, revealing the role of sex-related differences in AT2 expression (low expression in males and higher expression in females) in IL-10, IL-6, and IL-1β microglial levels.

IL-10 is a key anti-inflammatory cytokine that inhibits the release of pro-inflammatory cytokines and stimulates anti-inflammatory responses resulting in neuroprotection (Fouda et al., 2017; Khorooshi et al., 2020). IL-10 has been considered a key factor for balancing the immune response in the brain (Lobo-Silva et al., 2016). In different cell types, AT2 receptor activation induces the production of IL-10, which is inhibited by AT2 antagonists, appearing as the dominant cytokine mediating the AT2-induced anti-inflammatory response and the decrease in pro-inflammatory cytokines (Dhande et al., 2015; Khorooshi et al., 2020). Treatment with the AT2 agonist C21 increased the LPS-induced IL-10 levels and decreased inflammatory response, which was inhibited by treatment with neutralizing IL-10 antibody (Dhande et al., 2013; Fouda et al., 2017; Ismael & Ishrat, 2021), or in IL-10 KO mice (Khorooshi et al., 2020) or by the NO synthase inhibitor L-N^G-Nitro arginine methyl ester (L-NAME), revealing that the IL-10 mediates the AT2 anti-inflammatory effects, and that AT2-induced IL-10 production is largely NO dependent (Dhande et al., 2013). The AT2-induced up-regulation of IL-10 is mediated via a sustained, selective increase in ERK1/2 phosphorylation (Dhande et al., 2015). Although the precise link between NO production and IL-10 signaling is not totally clarified, it has been suggested that the signaling cascades activated by NO may result in downstream activation of mitogen-activated protein kinases (MAPKs) required for IL-10 production (Dhande et al., 2013; Li et al., 2006). It has been suggested that IL-10 mediates its anti-inflammatory actions through activation of the JAK1-STAT3 (Janus Kinase 1 Signal Transducer and Activator of Transcription 3) signaling pathway (Sabat et al., 2010).

IL-10 inhibits the production of the pro-inflammatory cytokines IL-6 and IL-1β. Treatment with the AT2 agonist C21 not only increased LPS-induced IL-10 levels, but decreased IL-6 levels, which was inhibited by treatment with neutralizing IL-10 antibodies or the NO synthase inhibitor L-NAME, revealing the inhibitory effect of IL-10 on IL-6 production (Dhande et al., 2013; Dhande et al., 2015). Several studies, including those using IL-10 deficient mice, have also shown that IL-10 inhibits IL-1β production in several cell types (Kim et al., 2021; Zhang et al., 2014), including microglia (Sun et al., 2019),

by inhibition of expression of pro-IL-1β and NLR family pyrin domain containing 3 (NLRP3) inflammasome components (Greenhill et al., 2014). However, other mechanisms independent of the increase in IL-10 may also be involved in the observed association between an increase in microglial AT2 expression and a decrease in IL-1β and IL-6 expression.

Sex differences in microglial AT2 receptor expression appear as a major factor contributing to sex differences in the neuroinflammatory microglial responses beyond the effects of circulating steroids in adult mice. The results of female brain masculinization and androgen depletion by orchiectomy do no suggest that the sex differences in AT2 expression are a consequence of the perinatal exposure to estrogens or differences in levels of androgens (i.e., androgen-induced downregulation of AT2 expression in males), and highlight the possibility of genomic reasons, probably related to sex chromosome complement effects. Some data in other tissues also support this possibility (Dadam et al., 2017; Denton, 2015; Pessoa et al., 2015). In an attempt to check epigenetic marks that would affect AT2 receptor gene expression, we implemented bisulfite DNA sequencing to track the methylation status in the promoter of the AT2 gene, and we found that the only CpG in the promoter is equally methylated in male and female samples. Nevertheless, although CpG methylation in promoters is usually associated with gene silencing, its role in the activity of CpG-poor promoter genes, such as this one, still remains elusive, with some studies indicating that they could remain expressed while methylated in a tissue-dependent context (Weber et al., 2007). Other epigenetic factors (i.e., histone modifications, histone variants, RNA coating) may contribute to the regulation of these genes, likely allowing them to evade X inactivation. Finally, there is also the possibility that sex complement effects in other X-linked genes may indirectly induce the observed upregulation of AT2 expression in females (Fish, 2008; Qi et al., 2021), and there is also the possibility that the Y-chromosome plays a repressive role in AT2 transcription by repressing the AT2 promotor (Araujo et al., 2015). All these possibilities remain to be studied and clarified in future studies specifically focused on this question.

In conclusion, the results confirm that sex differences may affect the outcome of neuroinflammation associated processes, and that sex differences in microglial AT2 expression play a major role. Although the results were obtained in mouse microglia, they further suggest that patient sex cannot be ignored when making therapeutical decisions. Sex differences in neuroinflammatory responses can be synergistically modulated by hormonal and environmental factors. However, it is known that a considerable number of immune-related genes are in the X chromosome, and that the number of scape genes is much higher in humans than in rodents. This may influence sex differences in the neuroinflammatory response, and it may be the case for microglial AT2 receptors. Further research is necessary to understand the mechanisms and role of X and Y chromosome genes in sex differences in neuroinflammation and particularly in the microglial function.

AUTHOR CONTRIBUTIONS

Pablo Garrido-Gil and **Maria Garcia-Garrote** performed microglial isolation and analysis. **Maria A. Pedrosa** performed RNA scope experiments. **Ana Pequeño-Valtierra**, **Jorge Rodríguez-Castro**, and **Daniel García-Souto** performed methylation studies. **Jose L. Labandeira-Garcia** and **Ana I. Rodríguez-Pérez**: fund acquisition, conceived, supervised the study and wrote the manuscript. All authors edited and approved the manuscript.

ACKNOWLEDGMENT

FUNDING INFORMATION

CONFLICT OF INTEREST

The authors declare that they have no competing interests.

DATA AVAILABILITY STATEMENT

The data sets used and/or analysed during the current study are available from the corresponding author on reasonable request.

ORCID

Ana I. Rodríguez-Pérez https://orcid.org/0000-0003-1354-8799
Jose L. Labandeira-Garcia https://orcid.org/0000-0002-8243-9791

REFERENCES

Acosta-Martinez, M. (2020). Shaping microglial phenotypes through estrogen receptors: Relevance to sex-specific neuroinflammatory responses to brain injury and disease. *The Journal of Pharmacology and Experimental Therapeutics*, *375*(1), 223–236. https://doi.org/10.1124/jpet.119.264598

Araujo, F. C., Milsted, A., Watanabe, I. K., Del Puerto, H. L., Santos, R. A., Lazar, J., Reis, F. M., & Prokop, J. W. (2015). Similarities and differences of X and Y chromosome homologous genes, SRY and SOX3, in regulating the renin-angiotensin system promoters. *Physiological Genomics*, *47*(5), 177–186. https://doi.org/10.1152/physiolgenomics.00138.2014

Arnold, A. P. (2020). Sexual differentiation of brain and other tissues: Five questions for the next 50 years. *Hormones and Behavior*, *120*, 104691. https://doi.org/10.1016/j.yhbeh.2020.104691

Bedecs, K., Elbaz, N., Sutren, M., Masson, M., Susini, C., Strosberg, A. D., & Nahmias, C. (1997). Angiotensin II type 2 receptors mediate inhibition of mitogen-activated protein kinase cascade and functional activation of SHP-1 tyrosine phosphatase. *Biochemical Journal*, *325*(Pt 2), 449–454. https://doi.org/10.1042/bj3250449

Bhat, S. A., Sood, A., Shukla, R., & Hanif, K. (2019). AT2R activation prevents microglia pro-inflammatory activation in a NOX-dependent manner: Inhibition of PKC activation and p47(phox) phosphorylation by PP2A. *Molecular Neurobiology*, *56*(4), 3005–3023. https://doi.org/10.1007/s12035-018-1272-9

Bordt, E. A., Ceasrine, A. M., & Bilbo, S. D. (2020). Microglia and sexual differentiation of the developing brain: A focus on ontogeny and intrinsic factors. *Glia*, *68*(6), 1085–1099. https://doi.org/10.1002/glia.23753

Carey, R. M., Jin, X., Wang, Z., & Siragy, H. M. (2000). Nitric oxide: A physiological mediator of the type 2 (AT2) angiotensin receptor. *Acta*

Physiologica Scandinavica, *168*(1), 65–71. https://doi.org/10.1046/j.1365-201x.2000.00660.x

Cora, M. C., Kooistra, L., & Travlos, G. (2015). Vaginal cytology of the laboratory rat and mouse: Review and criteria for the staging of the estrous cycle using stained vaginal smears. *Toxicologic Pathology*, *43*(6), 776–793. https://doi.org/10.1177/0192623315570339

Dadam, F. M., Cisternas, C. D., Macchione, A. F., Godino, A., Antunes-Rodrigues, J., Cambiasso, M. J., Vivas, L. M., & Caeiro, X. E. (2017). Sex chromosome complement involvement in angiotensin receptor sexual dimorphism. *Molecular and Cellular Endocrinology*, *447*, 98–105. https://doi.org/10.1016/j.mce.2017.02.041

de Gasparo, M., Catt, K. J., Inagami, T., Wright, J. W., & Unger, T. (2000). International union of pharmacology. XXIII. The angiotensin II receptors. *Pharmacological Reviews*, *52*(3), 415–472.

de Kloet, A. D., Wang, L., Ludin, J. A., Smith, J. A., Pioquinto, D. J., Hiller, H., Steckelings, U. M., Scheuer, D. A., Sumners, C., & Krause, E. G. (2016). Reporter mouse strain provides a novel look at angiotensin type-2 receptor distribution in the central nervous system. *Brain Structure & Function*, *221*(2), 891–912. https://doi.org/10.1007/s00429-014-0943-1

Denton, K. M. (2015). Angiotensin type 2 receptor: Hidden partner. *Hypertension*, *66*(2), 273–274. https://doi.org/10.1161/HYPERTENSIONAHA.115.05383

Dhande, I., Ali, Q., & Hussain, T. (2013). Proximal tubule angiotensin AT2 receptors mediate an anti-inflammatory response via interleukin-10: Role in renoprotection in obese rats. *Hypertension*, *61*(6), 1218–1226. https://doi.org/10.1161/HYPERTENSIONAHA.111.00422

Dhande, I., Ma, W., & Hussain, T. (2015). Angiotensin AT2 receptor stimulation is anti-inflammatory in lipopolysaccharide-activated THP-1 macrophages via increased interleukin-10 production. *Hypertension Research*, *38*(1), 21–29. https://doi.org/10.1038/hr.2014.132

Fatima, N., Patel, S. N., & Hussain, T. (2021). Angiotensin II type 2 receptor: A target for protection against hypertension, metabolic dysfunction, and organ remodeling. *Hypertension*, *77*(6), 1845–1856. https://doi.org/10.1161/HYPERTENSIONAHA.120.11941

Fish, E. N. (2008). The X-files in immunity: Sex-based differences predispose immune responses. *Nature Reviews. Immunology*, *8*(9), 737–744. https://doi.org/10.1038/nri2394

Fouda, A. Y., Pillai, B., Dhandapani, K. M., Ergul, A., & Fagan, S. C. (2017). Role of interleukin-10 in the neuroprotective effect of the angiotensin type 2 receptor agonist, compound 21, after ischemia/reperfusion injury. *European Journal of Pharmacology*, *799*, 128–134. https://doi.org/10.1016/j.ejphar.2017.02.016

Garrido-Gil, P., Rodriguez-Perez, A. I., Fernandez-Rodriguez, P., Lanciego, J. L., & Labandeira-Garcia, J. L. (2017). Expression of angiotensinogen and receptors for angiotensin and prorenin in the rat and monkey striatal neurons and glial cells. *Brain Structure & Function*, *222*(6), 2559–2571. https://doi.org/10.1007/s00429-016-1357-z

Garrido-Gil, P., Rodriguez-Perez, A. I., Lage, L., & Labandeira-Garcia, J. L. (2021). Estrogen deficiency and colonic function: Surgical menopause and sex differences in angiotensin and dopamine receptor interaction. *The Journals of Gerontology. Series A, Biological Sciences and Medical Sciences*, *76*(9), 1533–1541. https://doi.org/10.1093/gerona/glaa244

Garrido-Gil, P., Valenzuela, R., Villar-Cheda, B., Lanciego, J. L., & Labandeira-Garcia, J. L. (2013). Expression of angiotensinogen and receptors for angiotensin and prorenin in the monkey and human substantia nigra: An intracellular renin-angiotensin system in the nigra. *Brain Structure & Function*, *218*(2), 373–388. https://doi.org/10.1007/s00429-012-0402-9

Greenhill, C. J., Jones, G. W., Nowell, M. A., Newton, Z., Harvey, A. K., Moideen, A. N., Collins, F. L., Bloom, A. C., Coll, R. C., Robertson, A. A., Cooper, M. A., Rosas, M., Taylor, P. R., O'Neill, L. A., Humphreys, I. R., Williams, A. S., & Jones, S. A. (2014). Interleukin-10 regulates the inflammasome-driven augmentation of inflammatory arthritis and joint destruction. *Arthritis Research & Therapy*, *16*(4), 419. https://doi.org/10.1186/s13075-014-0419-y

Habib, P., & Beyer, C. (2015). Regulation of brain microglia by female gonadal steroids. *The Journal of Steroid Biochemistry and Molecular Biology*, *146*, 3–14. https://doi.org/10.1016/j.jsbmb.2014.02.018

Hafko, R., Villapol, S., Nostramo, R., Symes, A., Sabban, E. L., Inagami, T., & Saavedra, J. M. (2013). Commercially available angiotensin II At(2) receptor antibodies are nonspecific. *PLoS One*, *8*(7), e69234. https://doi.org/10.1371/journal.pone.0069234

Hakam, A. C., & Hussain, T. (2006). Angiotensin II AT2 receptors inhibit proximal tubular Na+-K+-ATPase activity via a NO/cGMP-dependent pathway. *American Journal of Physiology. Renal Physiology*, *290*(6), F1430–F1436. https://doi.org/10.1152/ajprenal.00218.2005

Han, J., Fan, Y., Zhou, K., Blomgren, K., & Harris, R. A. (2021). Uncovering sex differences of rodent microglia. *Journal of Neuroinflammation*, *18*(1), 74. https://doi.org/10.1186/s12974-021-02124-z

Hanamsagar, R., Alter, M. D., Block, C. S., Sullivan, H., Bolton, J. L., & Bilbo, S. D. (2017). Generation of a microglial developmental index in mice and in humans reveals a sex difference in maturation and immune reactivity. *Glia*, *65*(9), 1504–1520. https://doi.org/10.1002/glia.23176

Ismael, S., & Ishrat, T. (2021). Compound 21, a direct AT2R agonist, induces IL-10 and inhibits inflammation in mice following traumatic brain injury. *Neuromolecular Medicine*. https://doi.org/10.1007/s12017-021-08687-7

Jackson, L., Dong, G., Althomali, W., Sayed, M. A., Eldahshan, W., Baban, B., Johnson, M. H., Filosa, J., Fagan, S. C., & Ergul, A. (2020). Delayed administration of angiotensin II type 2 receptor (AT2R) agonist compound 21 prevents the development of post-stroke cognitive impairment in diabetes through the modulation of microglia polarization. *Translational Stroke Research*, *11*(4), 762–775. https://doi.org/10.1007/s12975-019-00752-5

Jackson, L., Eldahshan, W., Fagan, S. C., & Ergul, A. (2018). Within the brain: The renin angiotensin system. *International Journal of Molecular Sciences*, *19*(3), 876-898. https://doi.org/10.3390/ijms19030876

Joglar, B., Rodriguez-Pallares, J., Rodriguez-Perez, A. I., Rey, P., Guerra, M. J., & Labandeira-Garcia, J. L. (2009). The inflammatory response in the MPTP model of Parkinson's disease is mediated by brain angiotensin: Relevance to progression of the disease. *Journal of Neurochemistry*, *109*(2), 656–669. https://doi.org/10.1111/j.1471-4159.2009.05999.x

Kerr, N., Dietrich, D. W., Bramlett, H. M., & Raval, A. P. (2019). Sexually dimorphic microglia and ischemic stroke. *CNS Neuroscience & Therapeutics*, *25*(12), 1308–1317. https://doi.org/10.1111/cns.13267

Khorooshi, R., Tofte-Hansen, E. U., Tygesen, C., Montanana-Rosell, R., Limburg, H. L., Marczynska, J., Asgari, N., Steckelings, U. M., & Owens, T. (2020). Angiotensin AT2 receptor-induced interleukin-10 attenuates neuromyelitis optica spectrum disorder-like pathology. *Multiple Sclerosis: Clinical and Laboratory Research*, *26*(10), 1187–1196. https://doi.org/10.1177/1352458519860327

Kim, T. H., Yang, K., Kim, M., Kim, H. S., & Kang, J. L. (2021). Apoptosis inhibitor of macrophage (AIM) contributes to IL-10-induced anti-inflammatory response through inhibition of inflammasome activation. *Cell Death & Disease*, *12*(1), 19. https://doi.org/10.1038/s41419-020-03332-w

Lanfranco, M. F., Mocchetti, I., Burns, M. P., & Villapol, S. (2017). Glial- and neuronal-specific expression of CCL5 mRNA in the rat brain. *Frontiers in Neuroanatomy*, *11*, 137. https://doi.org/10.3389/fnana.2017.00137

Lawson, L. J., Perry, V. H., Dri, P., & Gordon, S. (1990). Heterogeneity in the distribution and morphology of microglia in the normal adult mouse brain. *Neuroscience*, *39*(1), 151–170. https://doi.org/10.1016/0306-4522(90)90229-w

Li, L. C., & Dahiya, R. (2002). MethPrimer: designing primers for methylation PCRs. *Bioinformatics*, *18*(11), 1427–1431. https://doi.org/10.1093/bioinformatics/18.11.1427

Li, Z., Zhang, G., Feil, R., Han, J., & Du, X. (2006). Sequential activation of p38 and ERK pathways by cGMP-dependent protein kinase leading to

activation of the platelet integrin alphaIIb beta3. *Blood*, 107(3), 965–972. https://doi.org/10.1182/blood-2005-03-1308

Lobo-Silva, D., Carriche, G. M., Castro, A. G., Roque, S., & Saraiva, M. (2016). Balancing the immune response in the brain: IL-10 and its regulation. *Journal of Neuroinflammation*, 13(1), 297. https://doi.org/10.1186/s12974-016-0763-8

Matavelli, L. C., Huang, J., & Siragy, H. M. (2011). Angiotensin AT(2) receptor stimulation inhibits early renal inflammation in renovascular hypertension. *Hypertension*, 57(2), 308–313. https://doi.org/10.1161/HYPERTENSIONAHA.110.164202

Mazure, C. M., & Swendsen, J. (2016). Sex differences in Alzheimer's disease and other dementias. *The Lancet. Neurology*, 15(5), 451–452. https://doi.org/10.1016/S1474-4422(16)00067-3

Okumura, M., Iwai, M., Ide, A., Mogi, M., Ito, M., & Horiuchi, M. (2005). Sex difference in vascular injury and the vasoprotective effect of valsartan are related to differential AT2 receptor expression. *Hypertension*, 46(3), 577–583. https://doi.org/10.1161/01.HYP.0000178564.14464.80

Pessoa, B. S., Slump, D. E., Ibrahimi, K., Grefhorst, A., van Veghel, R., Garrelds, I. M., Roks, A. J., Kushner, S. A., Danser, A. H., & van Esch, J. H. (2015). Angiotensin II type 2 receptor- and acetylcholine-mediated relaxation: Essential contribution of female sex hormones and chromosomes. *Hypertension*, 66(2), 396–402. https://doi.org/10.1161/HYPERTENSIONAHA.115.05303

Qi, S., Al Mamun, A., Ngwa, C., Romana, S., Ritzel, R., Arnold, A. P., McCullough, L. D., & Liu, F. (2021). X chromosome escapee genes are involved in ischemic sexual dimorphism through epigenetic modification of inflammatory signals. *Journal of Neuroinflammation*, 18(1), 70. https://doi.org/10.1186/s12974-021-02120-3

Rodriguez-Perez, A. I., Borrajo, A., Rodriguez-Pallares, J., Guerra, M. J., & Labandeira-Garcia, J. L. (2015). Interaction between NADPH-oxidase and Rho-kinase in angiotensin II-induced microglial activation. *Glia*, 63(3), 466–482. https://doi.org/10.1002/glia.22765

Rodriguez-Perez, A. I., Garrido-Gil, P., Pedrosa, M. A., Garcia-Garrote, M., Valenzuela, R., Navarro, G., Franco, R., & Labandeira-Garcia, J. L. (2020). Angiotensin type 2 receptors: Role in aging and neuroinflammation in the substantia nigra. *Brain, Behavior, and Immunity*, 87, 256–271. https://doi.org/10.1016/j.bbi.2019.12.011

Rodriguez-Perez, A. I., Valenzuela, R., Joglar, B., Garrido-Gil, P., Guerra, M. J., & Labandeira-Garcia, J. L. (2011). Renin angiotensin system and gender differences in dopaminergic degeneration. *Molecular Neurodegeneration*, 6(1), 58. https://doi.org/10.1186/1750-1326-6-58

Rodriguez-Perez, A. I., Valenzuela, R., Villar-Cheda, B., Guerra, M. J., & Labandeira-Garcia, J. L. (2012). Dopaminergic neuroprotection of hormonal replacement therapy in young and aged menopausal rats: Role of the brain angiotensin system. *Brain*, 135(Pt 1), 124–138. https://doi.org/10.1093/brain/awr320

Rompe, F., Artuc, M., Hallberg, A., Alterman, M., Stroder, K., Thone-Reineke, C., Reichenbach, A., Schacherl, J., Dahlof, B., Bader, M., Alenina, N., Schwaninger, M., Zuberbier, T., Funke-Kaiser, H., Schmidt, C., Schunck, W. H., Unger, T., & Steckelings, U. M. (2010). Direct angiotensin II type 2 receptor stimulation acts anti-inflammatory through epoxyeicosatrienoic acid and inhibition of nuclear factor kappaB. *Hypertension*, 55(4), 924–931. https://doi.org/10.1161/HYPERTENSIONAHA.109.147843

Ross, M. T., Grafham, D. V., Coffey, A. J., Scherer, S., McLay, K., Muzny, D., Platzer, M., Howell, G. R., Burrows, C., Bird, C. P., Frankish, A., Lovell, F. L., Howe, K. L., Ashurst, J. L., Fulton, R. S., Sudbrak, R., Wen, G., Jones, M. C., Hurles, M. E., ... Bentley, D. R. (2005). The DNA sequence of the human X chromosome. *Nature*, 434(7031), 325–337. https://doi.org/10.1038/nature03440

Sabat, R., Grutz, G., Warszawska, K., Kirsch, S., Witte, E., Wolk, K., & Geginat, J. (2010). Biology of interleukin-10. *Cytokine & Growth Factor Reviews*, 21(5), 331–344. https://doi.org/10.1016/j.cytogfr.2010.09.002

Sedgwick, J. D., Schwender, S., Imrich, H., Dorries, R., Butcher, G. W., & ter Meulen, V. (1991). Isolation and direct characterization of resident microglial cells from the normal and inflamed central nervous system. *Proceedings of the National Academy of Sciences of the United States of America*, 88(16), 7438–7442. https://doi.org/10.1073/pnas.88.16.7438

Sun, Y., Ma, J., Li, D., Li, P., Zhou, X., Li, Y., He, Z., Qin, L., Liang, L., & Luo, X. (2019). Interleukin-10 inhibits interleukin-1beta production and inflammasome activation of microglia in epileptic seizures. *Journal of Neuroinflammation*, 16(1), 66. https://doi.org/10.1186/s12974-019-1452-1

Syrett, C. M., & Anguera, M. C. (2019). When the balance is broken: X-linked gene dosage from two X chromosomes and female-biased autoimmunity. *Journal of Leukocyte Biology*, 106(4), 919–932. https://doi.org/10.1002/JLB.6RI0319-094R

Tukiainen, T., Villani, A. C., Yen, A., Rivas, M. A., Marshall, J. L., Satija, R., Aguirre, M., Gauthier, L., Fleharty, M., Kirby, A., Cummings, B. B., Castel, S. E., Karczewski, K. J., Aguet, F., Byrnes, A., GTEx Consortium, Lappalainen, T., Regev, A., Ardlie, K. G., ... MacArthur, D. G. (2017). Landscape of X chromosome inactivation across human tissues. *Nature*, 550(7675), 244–248. https://doi.org/10.1038/nature24265

VanRyzin, J. W., Marquardt, A. E., Argue, K. J., Vecchiarelli, H. A., Ashton, S. E., Arambula, S. E., Hill, M. N., & McCarthy, M. M. (2019). Microglial phagocytosis of newborn cells is induced by endocannabinoids and sculpts sex differences in juvenile rat social play. *Neuron*, 102(2), 435–449e436. https://doi.org/10.1016/j.neuron.2019.02.006

Villa, A., Gelosa, P., Castiglioni, L., Cimino, M., Rizzi, N., Pepe, G., Lolli, F., Marcello, E., Sironi, L., Vegeto, E., & Maggi, A. (2018). Sex-specific features of microglia from adult mice. *Cell Reports*, 23(12), 3501–3511. https://doi.org/10.1016/j.celrep.2018.05.048

Villa, A., Vegeto, E., Poletti, A., & Maggi, A. (2016). Estrogens, neuroinflammation, and neurodegeneration. *Endocrine Reviews*, 37(4), 372–402. https://doi.org/10.1210/er.2016-1007

Villapol, S., Loane, D. J., & Burns, M. P. (2017). Sexual dimorphism in the inflammatory response to traumatic brain injury. *Glia*, 65(9), 1423–1438. https://doi.org/10.1002/glia.23171

Wang, X., Tu, J., Jiang, J., Zhang, Q., Liu, Q., Korner, H., Wu, J., Wu, H., & Wei, W. (2020). Angiotensin II type 2 receptor modulates synovial macrophage polarization by inhibiting GRK2 membrane translocation in a rat model of collagen-induced arthritis. *The Journal of Immunology: Official Journal of the American Association of Immunologists*, 205(11), 3141–3153. https://doi.org/10.4049/jimmunol.2000561

Weber, M., Hellmann, I., Stadler, M. B., Ramos, L., Paabo, S., Rebhan, M., & Schubeler, D. (2007). Distribution, silencing potential and evolutionary impact of promoter DNA methylation in the human genome. *Nature Genetics*, 39(4), 457–466. https://doi.org/10.1038/ng1990

Zang, C., Yang, H., Wang, L., Wang, Y., Bao, X., Wang, X., & Zhang, D. (2019). A novel synthetic derivative of phloroglucinol inhibits neuroinflammatory responses through attenuating Kalirin signaling pathway in murine BV2 microglial cells. *Molecular Neurobiology*, 56(4), 2870–2880. https://doi.org/10.1007/s12035-018-1233-3

Zhang, J., Fu, S., Sun, S., Li, Z., & Guo, B. (2014). Inflammasome activation has an important role in the development of spontaneous colitis. *Mucosal Immunology*, 7(5), 1139–1150. https://doi.org/10.1038/mi.2014.1

SUPPORTING INFORMATION

Additional supporting information can be found online in the Supporting Information section at the end of this article.